Model-based estimation of negative inspiratory driving pressure in patients receiving invasive NAVA mechanical ventilation

Jennifer L. Knopp*[1], J. Geoffrey Chase[1], Kyeong Tae Kim[1], Geoffrey M. Shaw[2]

1. Department of Mechanical Engineering, University of Canterbury, Private Bag 4800, Christchurch, New Zealand

2. Department of Intensive Care, Christchurch Hospital, Christchurch, Private Bag 4710, New Zealand

***Corresponding Author**:

Jennifer L. Knopp
Department of Mechanical Engineering
University of Canterbury
Private Bag 4800
Christchurch 8140
New Zealand
Email: Jennifer.knopp@canterbury.ac.nz
Phone: +64 3 3692411

ABSTRACT:

Background: Optimisation of mechanical ventilation (MV) and weaning requires insight into underlying patient breathing effort. Current identifiable models effectively describe lung mechanics, such as elastance (E) and resistance (R) at the bedside in sedated patients, but are less effective when spontaneous breathing is present. This research derives and regularises a single compartment model to identify patient-specific inspiratory effort.

Methods: Constrained second-order b-spline basis functions (knot width 0.05 seconds) are used to describe negative inspiratory drive (Pp, cmH_2O) as a function of time. Breath-breath Pp are identified with single E and R values over inspiration and expiration from n=20 breaths for N=22 patients on NAVA ventilation. Pp is compared to measured electrical activity of the diaphragm (Eadi) and published results.

Results: Average per-patient root-mean-squared model fit error was (median [interquartile range, IQR]) 0.9 [0.6–1.3] cmH_2O, and average per-patient median Pp was -3.9 [-4.5– -3.0] cmH_2O, with range -7.9 – -1.9 cmH_2O. Per-patient E and R were 16.4 [13.6–21.8] cmH_2O/L and 9.2 [6.4–13.1] $cmH_2O.s/L$, respectively. Most patients showed an inspiratory volume threshold beyond which Pp started to return to baseline, and Pp at peak Eadi (end-inspiration) was often strongly correlated with peak Eadi (R^2=0.25-0.86). Similarly, average transpulmonary pressure was consistent breath-breath in most patients, despite differences in peak Eadi and thus peak airway pressure.

Conclusions: The model-based inspiratory effort aligns with electrical muscle activity and published studies showing neuro-muscular decoupling as a function of pressure and/or volume. Consistency in coupling/dynamics were patient-specific. Quantification of patient and ventilator work of breathing contributions may aid optimisation of MV modes and weaning.

Keywords: Spontaneous breathing, inspiratory effort, physiological modelling, lung mechanics

Abbreviations: ARDS: acute respiratory distress syndrome; Eadi: electrical activity of the diaphragm, MV: mechanical ventilation; NAVA: neutrally adjusted ventilator assist; PEEP: positive end expiratory pressure; PIP: peak inspiratory pressure; PS: pressure support; VILI: ventilator induced lung injury; WOB: work of breathing;

INTRODUCTION

Mechanical Ventilation (MV) is a core intensive care therapy, supporting breathing in patients with respiratory failure or acute respiratory distress syndrome (ARDS). However, significant inter- and intra- patient variability in response to care makes MV delivery difficult, and sub-optimal MV can cause ventilator induced lung injury (VILI) [1-4]. Thus, MV practice is not standardised and typically seeks to provide breathing support, maintain adequate gas exchange, and minimise VILI [1, 5].

Model-based methods may help personalise and optimise MV therapy by providing direct and indirect assessment of patient-specific respiratory mechanics in real-time at the bedside [6-8]. In particular, patient-specific positive end expiratory pressure (PEEP) is associated with VILI through the provision of excessive or insufficient baseline pressure during MV, through either damagingly high peak inspiratory pressures (PIP) [9, 10] or insufficient maintenance of alveolar recruitment and atelectrauma [11, 12]. Optimisation of PEEP via model-based methods is proposed as a lung protective strategy [6, 8, 13], and is supported by results showing ventilation at minimum patient-specific elastance reduces mortality [14, 15].

Current model-based methods for use at the bedside commonly utilise relatively simple, readily identifiable compartment models [6, 16-18] , where the lungs and airways are modelled as functions of respiratory elastance (E) and airway resistance (R). they are effective in fully sedated patients [6], where the work of breathing (WOB) is done by the ventilator and passive respiratory mechanics (E and R) can be identified from airway pressure and flow profiles. Spontaneous breathing during MV, where the patient performs some proportion of the WOB either in or out of synchrony with the ventilator, can mask identification of these respiratory parameters [19-21], complicating model-based analyses and protocols.

Spontaneous breathing during ventilation has harmful or beneficial impacts, depending on how well it synchronises with the ventilator. One review summarises how spontaneous breathing can result in ventilator-patient asynchrony and/or injury [22-24], particularly during controlled ventilation. In contrast, other studies show assisting spontaneous breathing may be beneficial for recovery and weaning [23], lowering ventilator induced diaphragm dysfunction [25] and improving pulmonary function and gas exchange [26, 27]. In some contexts, such as the neonatal intensive care unit, full sedation is uncommon, and patient-triggered ventilation modes are used to synchronise with and support the patient's own breathing efforts [28]. Equally, adult intensive care unit patients are increasingly ventilated in assisted breathing modes with spontaneous breathing, particularly as patients evolve towards weaning of ventilator support. Thus, spontaneous breathing during MV is increasingly common in practice, and methods for monitoring and assessing patient-ventilator interaction and patient breathing effort every breath are necessary.

Pressure support (PS, described in [29]) and neutrally adjusted ventilator assist (NAVA, described in [24]) are two common MV modes to support spontaneous breathing. In PS, the ventilator supports pressure to meet a set PIP in response to flow or pressure triggering. NAVA utilises the electrical activity of the diaphragm (Eadi) to trigger breaths and provide PIP in proportion to the peak Eadi signal. NAVA can improve patient-ventilator synchrony [30, 31] and matching tidal volume to effort [32], but requires additional invasive sensors. In either mode, the level of spontaneous breathing effort versus ventilator provided WOB cannot be quantified [29], leaving a significant gap in insight.

The proportion of the WOB performed by the ventilator and the patient is a function of the PS or NAVA level. At higher levels (and thus higher PIP) esophageal pressure measurements have shown decreased patient inspiratory drive, and thus decreased patient driven WOB, compared to ventilation at lower levels [29, 33-38]. This behaviour is termed ventilator unloading, where the greater the MV support provided, the lower the patient's WOB effort, as a greater proportion of the total WOB is 'unloaded'

onto the ventilator [29, 33-38]. Ventilator unloading means even where the neuromuscular coupling linking the Eadi electrical signal to muscular spontaneous breathing effort is good, the relationship between Eadi and actual spontaneous breathing effort [24] is non-linear [33], function of multiple inputs, patient-specific, and thus very difficult to ascertain. Measurement of esophageal pressures, a surrogate for pleural pressure, and thus diaphragmatic breathing effort [39], requires additional invasive measurements and equipment, and is not clinically feasible in standard care.

In addition, there is uncertainty around the optimum level of ventilator assist [40], where the aim is to sufficiently ventilate the patient, while balancing fatigue or patient spontaneous breathing capacity against complications from muscle atrophy. Trends in tidal volume, PIP, and Eadi suggest a region of NAVA levels where a patients 'preferred' tidal volume is achieved with differences in ventilator-patient WOB distribution [24, 40]. Lower NAVA levels (with lower tidal volumes) than this region have higher Eadi signal, suggesting insufficient ventilation increasing respiratory drive, while higher levels result in higher PIP and tidal volume, suggesting over-compensation [24, 40]. Since, optimising spontaneous breathing and the level of support in MV may improve weaning success, there is a need for a simple non-invasive measure of the negative pressure generation during spontaneous breathing effort to provide insight into patient respiratory effort to guide MV and weaning.

This study presents model-based methods to estimate breath-to-breath negative driving pressures, reflecting patient-specific and breath-specific WOB due to spontaneous breathing. These inspiratory efforts are compared to Eadi from NAVA MV patients as a first model-validation. The overall aim is to develop model-based methods based off the pressure/flow measurements available at the bedside to describe spontaneous breathing effort, thus clarifying the underlying patient respiratory mechanics and providing insight for ventilation optimisation and weaning at the bedside.

METHODS

2.1 Patients and Data

Intubated intensive care patients treated with PS ventilation were prospectively recruited under informed consent to a trial on patient-ventilator synchrony at the University Hospital of Geneva (Switzerland) and Cliniques Universitaires St-Luc (Brussels, Belgium) [41]. Exclusion criteria included: 1) severe hypoxia requiring FIO2>= 50%; 2) hemodynamic instability; 3) known esophageal problems such as hiatal hernia or esophogeal varicosities; 4) active upper gastro-intestinal bleeding or other contraindication to the insertion of a naso-gastric tube; 5) age <=16 years old; poor short term prognosis defined as high risk of death in next 7 days; and 7) neuro-muscular disease. All patients were ventilated on a Servo-I ventilator (Maquet, Solna, Sweden) capable of delivering MV under PS and NAVA modes. Standard nasogastric tubes were replaced with NAVA tubes in patients after study recruitment. The study protocol was approved by the ethics committees of both participating centres.

The prospective study included two phases, where patient data was first recorded for 20 minutes (~300-500 breaths) under the PS mode with clinician determined ventilator settings. The patient was then switched to NAVA with the NAVA level set so the PIP was similar to the level under the previous PS ventilation based on ventilator waveform visualisation, and another 20 minutes of data was recorded. All other ventilator settings for PS and NAVA were kept constant. During both periods, pressure, flow, and Eadi were acquired from the Servo-I ventilator and recorded at 100Hz by Servo-tracker V4.0 (Maquet, Solna, Sweden). In this preliminary study of spontaneous breathing effort, only the NAVA data is used in model-based analyses as ventilator-delivered pressure and flow is more dynamically influenced by spontaneous breathing in comparison to PS data.

2.2 Model

Pressures within the respiratory system and wider anatomy, summarised in Figure 1, can be simplified down to several basic components: pressure at the airway opening (P_{aw}), pressure within the lung

alveoli (P_a), pleural pressure (P_p), and gastric pressure (P_g). During spontaneous breathing, diaphragm activation generates a pressure difference between the pleural and gastric spaces (ΔP_{Di}), which in turn causes a trans-pulmonary pressure difference (ΔP_{TP}) driving lung expansion and inspiratory flow.

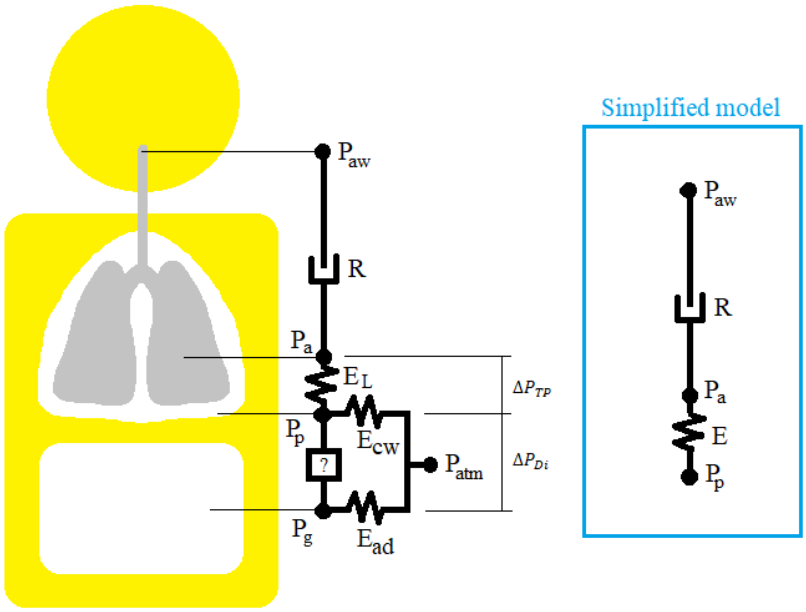

Figure 1: Compartment modelling of the respiratory system. P_{aw} is airway pressure, P_a is alveolar pressure, P_p is pleural pressure, P_g is the gastric/abdominal pressure, and P_{atm} is atmospheric pressure. ΔP_{TP} is thus the trans-pulmonary pressure, and ΔP_{Di} the trans-diaphragmatic pressure. Lung, chest wall, and abdominal tissue elastances/stiffnesses are modelled as springs (E_L, E_{CW}, E_ad), while airway resistance is proportional to flow as per the damping/resistance co-efficient R.

The pressure drop across the airways can be modelled proportional to flow:

$$P_{aw} = P_a + RQ \tag{1}$$

Where Q is flow (mL/s) and R is airway resistance (cmH_2O.s/mL). Trans-pulmonary pressure, assuming negligible tissue inertial effects, is a function of the elastic recoil of the lung:

$$\Delta P_{TP} = P_a - P_p = E_L V \tag{2}$$

Where E_L is lung elastance (cmH₂O/mL), and V is volume (L). Plural pressure can in turn be defined as a function of trans-diaphragmatic pressure and chest wall recoil:

$$P_p = \left(P_g + \Delta P_{Di}\right) + E_{CW} V_p \quad (3)$$

Where E_{CW} is chest wall elastance (cmH₂O/mL), and V_p is the volume of the pleural space (L). Thus, substituting Equation (3) into Equation (2), and rearranging in terms of P_a yields:

$$P_a = E_L V + \left(P_g + \Delta P_{Di}\right) + E_{CW} V_p \quad (4)$$

If volumes are set relative to end expiratory volumes, and the volumetric change is assumed similar between the lung and pleural cavity, Equation 4 can be grouped and simplified to:

$$P_a = EV + \widehat{P_p} \quad (5)$$

Where $\widehat{P_p} = P_g + \Delta P_{Di}$ relative to a baseline pressure at end expiration at the set PEEP, and the lung and chest wall elastances can be combined into a single overall elastance, $E = E_L + E_{CW}$.

Thus, Equation 1 can be redefined:

$$P_{aw} = EV + RQ + \widehat{P_p} \quad (6)$$

Where $\widehat{P_p}$ is the pressure change in the pleural space due to diaphragmatic action, and the initial two terms are the same as those in the well-known single compartment model [17].

In assisted ventilation of spontaneous breathing with an applied PEEP, Equation (6) becomes:

$$P_{aw} = PEEP + EV + RQ + \widehat{P_p} \quad (7)$$

Where V is tidal volume above end-expiratory volume at the current PEEP. Equation (7) represents the addition of a spontaneous breathing term to the well-used and clinically validated single compartment model [6, 16-18].

Pleural driving pressure, $\widehat{P_p}$, is unknown and cannot be measured non-invasively. However, it can be modelled using b-spline functions, rather than a set inspiratory effort shape function [42], due to multifactorial and time-varying contributions to inspiratory effort. B-splines are defined over time, per [43, 44], for first ($d = 0$) and higher orders ($d > 0$, recursively defined):

$$\Phi_{\mathrm{i,0}}(t) = f(x) = \begin{cases} 1, & T_i < t < T_i + 1 \\ 0, & otherwise \end{cases} \quad (8)$$

$$\Phi_{\mathrm{i,d}}(t) = \frac{t - T_i}{T_{i+d} - T_i}\Phi_{\mathrm{i,d-1}}(t) + \frac{T_{i+d+1} - t}{T_{i+d+1} - T_{i+1}}\Phi_{\mathrm{i+1,d-1}}(t) \quad for\ d \geq 1 \quad (9)$$

Where T_i are equally spaced division points in time, also known as knots. A spline is non-zero on $d + 1$ knot spans, and the functions sum to 1.0 at all points in time. In this analysis, 2nd order splines are used to describe $\widehat{P_p}$ during inspiration:

$$\widehat{P_p} = \sum_{i=1}^{M} -P_{s,i}\Phi_{i,2}(t) \quad (10)$$

Where $P_{s,i}$ are constant valued coefficients identified from measured data, and 2nd order (d=2) splines with a knot width (k_w) of 0.05 seconds and a maximum spline timespan, are defined for inspiration:

$$C = k_w \times \text{ceiling}\left(\frac{T_{insp}}{k_w}\right) \tag{11}$$

$$M = T_{max}/k_w + d;$$

Where T_{max} is the maximum basis-function time definition, and represents the measured inspiratory time, T_{insp}, rounded up to the nearest multiple of the knot width (k_w). There are thus *M* basis functions over a time period from 0-T_{max}.

The b-splines and an example identified result from data are shown in Figure 2, where Figure 2b shows how the weighted sum of splines can be used to describe non-standard shapes for inspiratory driving pressure. B-splines are constrained in this analysis to a physiological definition of spontaneous breathing, which requires negative pressure generation, thus yielding the negative sign before $P_{s,i}$ in Equation (10).

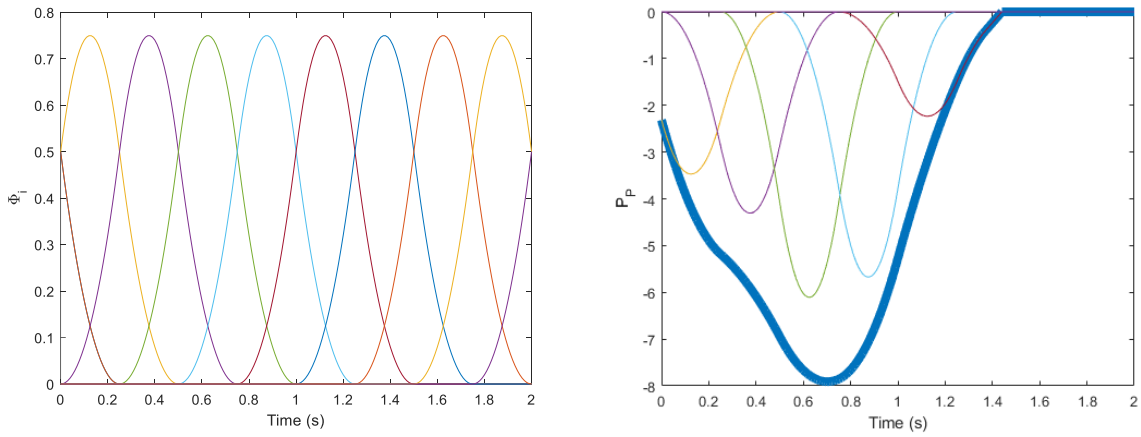

a) b)

Figure 2: a) Second order b-spline functions (d=2, 10 knots, 2 seconds) are used to b) model breathing effort as a sum of weighted splines. Note in this example the positive b-spline functions describe negative inspiratory effort through identification of negative values of the coefficients.

2.3 Parameter Identification

Equations (7)-(10) can be combined to yield:

$$P_{aw} = PEEP + EV(t) + R(t)Q(t) - \sum_{i=1}^{10} P_{s,i}\Phi_{i,2}(t) \tag{12}$$

Where for this analysis E and R are constants (cmH_2O/mL and $cmH_2O.s/mL$), per [6]. Linear least squares regression is used to identify lung mechanical properties (E, R) and patient breathing effort $(\hat{P}_p)$ by identifying the $P_{s,i}$ terms from n breaths using a system of equations defined:

$$Ax = b \tag{13}$$

$$A = \begin{bmatrix} V_1(t), & Q_1(t), & -\Phi_{1,1,2}(t), \dots -\Phi_{1,M,2}(t), & [0]_{(n-1)\times M} \\ \vdots & & & \vdots \\ V_n(t), & Q_n(t), & [0]_{(n-1)\times M}, & -\Phi_{n,1,2}(t), \dots -\Phi_{n,M,2}(t) \end{bmatrix}$$

$$b = \begin{bmatrix} P_{aw,1}(t) \\ \vdots \\ P_{aw,n}(t) \end{bmatrix} - PEEP$$

$$x = \left[E, R, P_{s,1,1} \dots P_{s,1,M}, \dots, P_{s,n,1}, \dots, P_{s,n,M}\right]^T$$

Where $P_{aw}(t)$ and $Q(t)$ are measured by the ventilator, and $V(t)$ is integrated on a breath-by-breath basis from measured flow, $Q(t)$.

A single set of passive mechanical properties (E, R) is identified across all n breaths as these properties are expected to remain constant over this period. Patient inspiratory breathing effort $(\hat{P}_p)$ is identified every breath. Least squares regression is done using Matlab's (Mathworks, Natick, MA, USA) lsqlin function, with E, R, with the first 75% of M b-spline function coefficients, $P_{s,i}$, for each breath constrained to be positive. The remaining 25% of b-spline functions per breath are not constrained according to the least squares definition in Equation (12), which enables end-inspiratory patient effort

against the ventilator to be captured, if present. The choice of constant (E, R) and constraining some values of $P_{s,i} > 0$, regularises the identification problem in Equation (13) and ensure it is identifiable.

In this analysis, the first $n = 20$ breaths are used, and parameters identified simultaneously per Equation (12). Both inspiration and expiration data is used, as the predominantly passive expiratory dynamics improve identification of 'passive' lung mechanic properties [18]. Inspiration onset is defined as more than 0.3 second of positive flow following negative expiratory flow. During parameter identification expiration data is truncated by discarding the first 5 data points, where the sudden pressure drop is predominantly a function of ventilator and breathing circuit mechanics. To ensure data is not heavily weighted towards expiration, which is approximately twice as long as inspiration, expiration data is also truncated at the end to flows greater than 10% of the maximum expiratory flow. This latter truncation also ensures expiration data predominantly contains the dynamic, lung mechanics induced portion of expiration and excludes the extended end-expiration period of relatively very low, constant pressure and airflow.

2.4 Analyses

The model was identified for the first 20 breaths from each patient's time on NAVA ventilation. Inspiration was defined as positive flow resulting in a lung volume change of greater than 50mL, and expiration is the period of negative flow following inspiration. Breaths where end expiratory volume was more than 50 mL different from the expected 0 mL were discarded, due to assumptions of air leaks and/or active expiratory effort causing greater expiration than inspiration. Patient-initiated end of inspiration ($t_{i,end-p}$) is defined as post peak-Eadi, while ventilator delivered end-inspiration (end of positive flow, $(t_{i,end-v})$ usually occurs once Eadi has dropped to ~70-80% of its peak value.

Identification fit error is reported as median [IQR] per-patient RMS error. NAVA efficacy is assessed via correlation of PIP with peak Eadi. The correlation of tidal volume with PIP (V_t vs. PIP) reflects

variability in delivered volume due to patient-specific and breath-specific variability in breathing effort on top of ventilator-delivered pressure, where a perfect correlation would be expected where there was no inspiratory effort for a primarily elastance-characterised (EV) pressure response. Equally, strongly consistent inspiratory effort for a given Eadi (and thus PIP under NAVA) could also result in a high V_t vs. PIP correlation, so this correlation more strongly indicates patients with variability in neuro-muscular coupling. Linear regression is used, and y-intercepts are not constrained to go through (0,0).

Model-based negative inspiratory effort ($\hat{P}_p$) is compared to Eadi, both as time-dependant profiles within inspiration ($t = 0 \rightarrow t_{i,end-p}$), and values at peak Eadi ($Eadi_{peak}$ vs. $\hat{P}_p|_{peak\ Eadi}$), to assess model outcomes against expected behaviours. Comparison of normalised $\hat{P}_p$ to inspired volume over patient-inspiration ($t = 0 \rightarrow t_{i,end-p}$) is used to examine consistency in decoupling of muscle activity (pressure generated, $\hat{P}_p$) from the electrical activity as a function of volume (and thus stress/strain). Finally, mean $\hat{P}_p$ over patient-inspiration is plotted against mean $P_a = P_{aw} - RQ$, to assess whether outcomes fall along lines of constant trans-pulmonary pressure, as per the analysis of [37].

3.0 Results

3.1 Model outcomes

Patient mechanical ventilation outcomes are given in Table 1. The model was fit to 20 breaths from each patient, with median [IQR] per-patient RMS error of 0.9 [0.6 – 1.3] cmH_2O. RMS error over ventilator-driven inspiration ($t = 0 \rightarrow t_{i,end-v}$) was slightly smaller, with median [IQR] RMS error 0.3 [0.2 – 0.9] cmH_2O, as would be expected when using b-spline functions to describe breath-to-breath inspiratory effort in addition to passive mechanics. Peak residual error in expiration typically occurred near peak expiratory flow, and likely reflects lung tissue relaxation time-constants not captured in the single compartment model [45-47].

A typical breath with identified model fit is shown for each patient in in Figure 2, along with negative inspiratory effort ($\hat{P}_p$) and model residuals. Mechanical ventilation and model-based outcomes are summarised in Table 2. B-spline function outcomes indicate spontaneous breathing was present, as would be expected for NAVA or any assisted breathing mode ventilation. Breath-to-breath peak modelled $\hat{P}_p$ is given in Table 2, where the per-patient median ranged from -1.9 to -7.9 cmH_2O. The shape of b-spline $\hat{P}_p$ outcomes also matched net expected pleural pressure variations.

The per-patient correlation of PIP delivered with peak Eadi in Table 2 is very high (R^2 = 0.71-0.99), as would be expected by NAVA ventilation design [24]. Correlation of PIP with tidal volume resulted in regression constants that varied from 0.1-0.93 with a median R^2 = 0.68. Patients with a V_t vs. PIP R^2 value less than 0.68 had lower, but not statistically different, R^2 values for $Eadi_{peak}$ vs. $\hat{P}_p|_{peak\ Eadi}$ than those with values higher than 0.69 (median [IQR]: 0.47 [0.36 – 0.62] vs. 0.67 [0.44 - 0.80], p = 0.16), but E and peak $\hat{P}_p$ were not different (17.4 [10.1 – 21.4] vs. 16.1 [14.6 – 22.5] cmH_2O/mL, p = 0.69, and -3.9 [-4.1 - -2.4] vs. -4.0 [-4.8 - -3.8] cmH_2O, p=0.26, respectively).

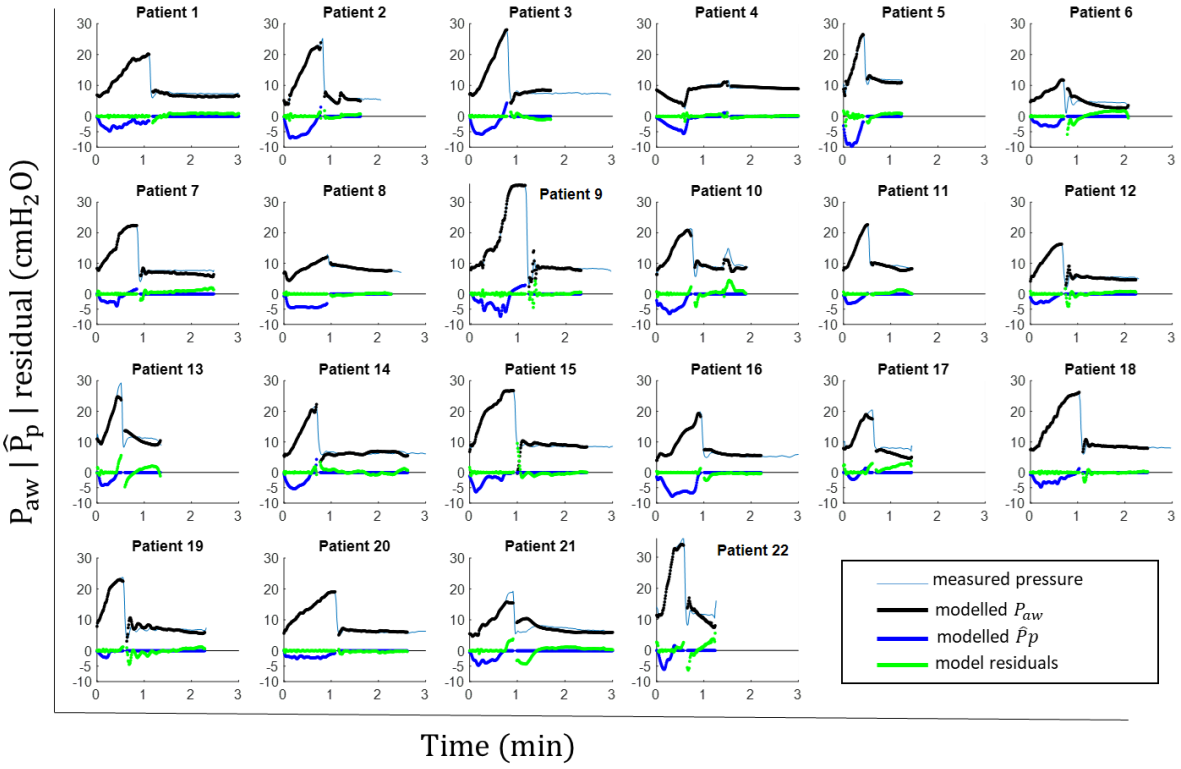

Figure 2: A typical model-fit to ventilator data for each patient. 'Typical' breaths are selected for representing the middle values of PIP, Vt, and negative inspiratory pressure ($\hat{P}_p$).

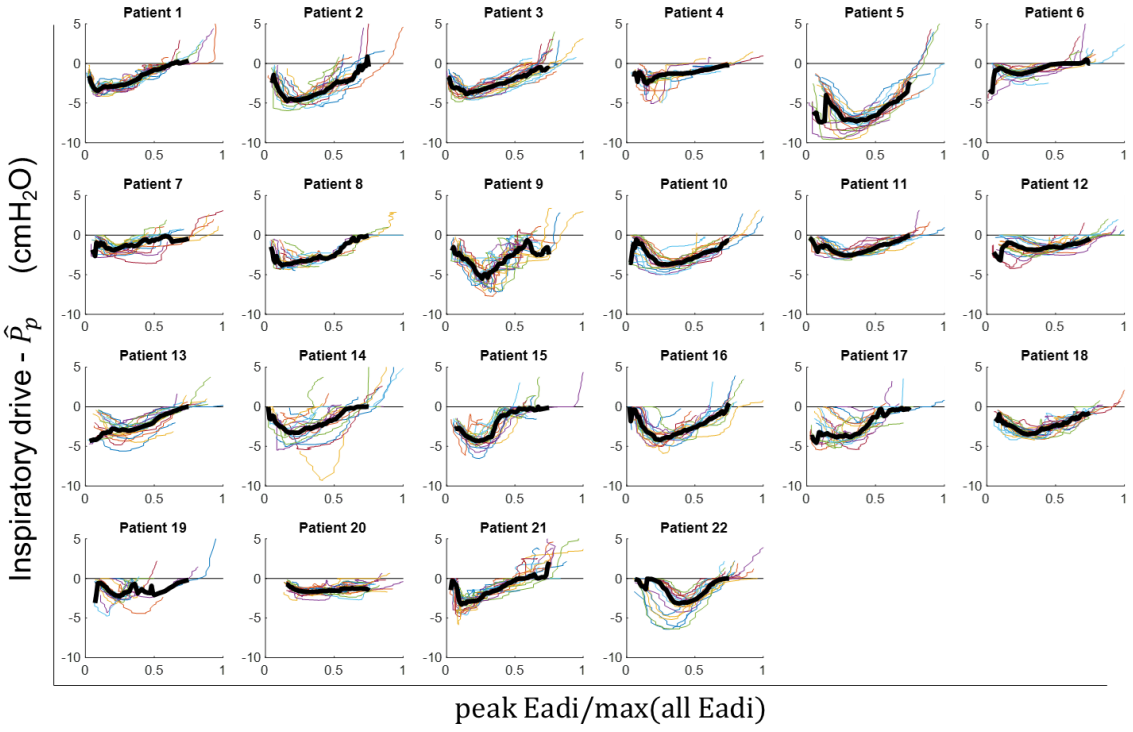

Figure 3: Negative inspiratory pressure ($\hat{P}_p$) for each breath vs. normalised Eadi for 20 NAVA breaths in a single model identification (n = 20) for each patient. Bold lines show the median inspiratory drive across Eadi.

Negative inspiratory drive was non-linear, and overall generally consistent within a patient across 20 breaths, with Eadi, as shown in Figure 3. It should be noted the model fitting process in Equation (12) is independent of Eadi. Non-linearity in the form of a maximum (negative) inspiratory pressure drive followed by a reduction in inspiratory drive as Eadi continues to rise, suggests complexities in the transformation of electrical signals to muscular diaphragm action, and may indicate the presence of ventilator unloading.

Correlation of pleural pressure ($\hat{P}_p$) with Eadi, reflecting achieved negative inspiratory effort from a neural input signal, is presented in Table 3 and Figure 4. Most patients showed a reduction in the breath-to-breath negative inspiratory driving pressure (became more positive) with increasing Eadi peaks, and R^2 values varied between 0.25 and 0.86, with median 0.55. Comparison of patients above and below the median for R^2 showed no difference in per-patient median peak $\hat{P}_p$ (-4 [-4.5 - -3.8] vs. -3.8 [-4.1 - -2.8] cmH_2O, p=34), E (16.1 [13.7-18.4] vs. 16.7 [12.3 – 23.3] cmH_2O/mL, p= 0.82) or R (8.4 [6.6 – 11.7] vs. 9.9 [6.3 – 13.4] cmH2O.s/mL, p = 0.74) The reduction in negative inspiratory driving pressure at peak Eadi with increasing Eadi is hypothesised to result from ventilator unloading, where an increasing proportion of elastic work is done by ventilator at higher support levels.

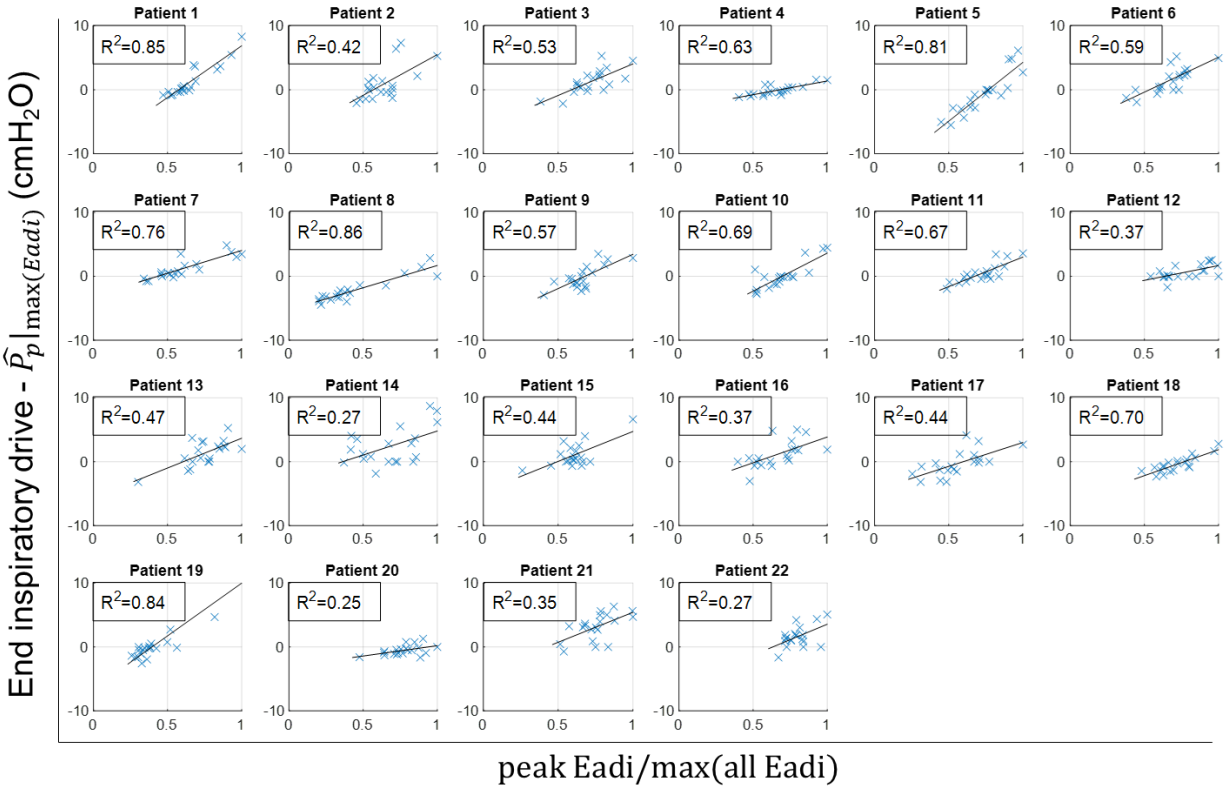

Figure 4: End inspiratory drive as reflected in negative inspiratory $\hat{P}_p|_{max\,(Eadi)}$ vs. peak neural electrical signal (Eadi). Results are for a single identification over 20 breaths.

Normalised b-spline function outcomes, $\hat{P}_p$, are plotted against volume for each of the 20 breaths (Figure 5) to assess any consistency in ventilator unloading onset. Results are the same, with the x-axis scaled, if plotted against trans-pulmonary pressure ($P_{TP} = EV(t)$). Most patients had a narrow range of lung volumes beyond which negative pressure generation started to drop off. Correspondingly, Figure 6 shows average inspiratory effort vs. average alveolar pressure tends to fall along lines of constant trans-pulmonary pressure. This outcome suggests ventilator unloading within a breath is based on physiological feedback systems around stress and/or strain (surrogate: volume), where the unloading onset is likely PEEP and NAVA level specific.

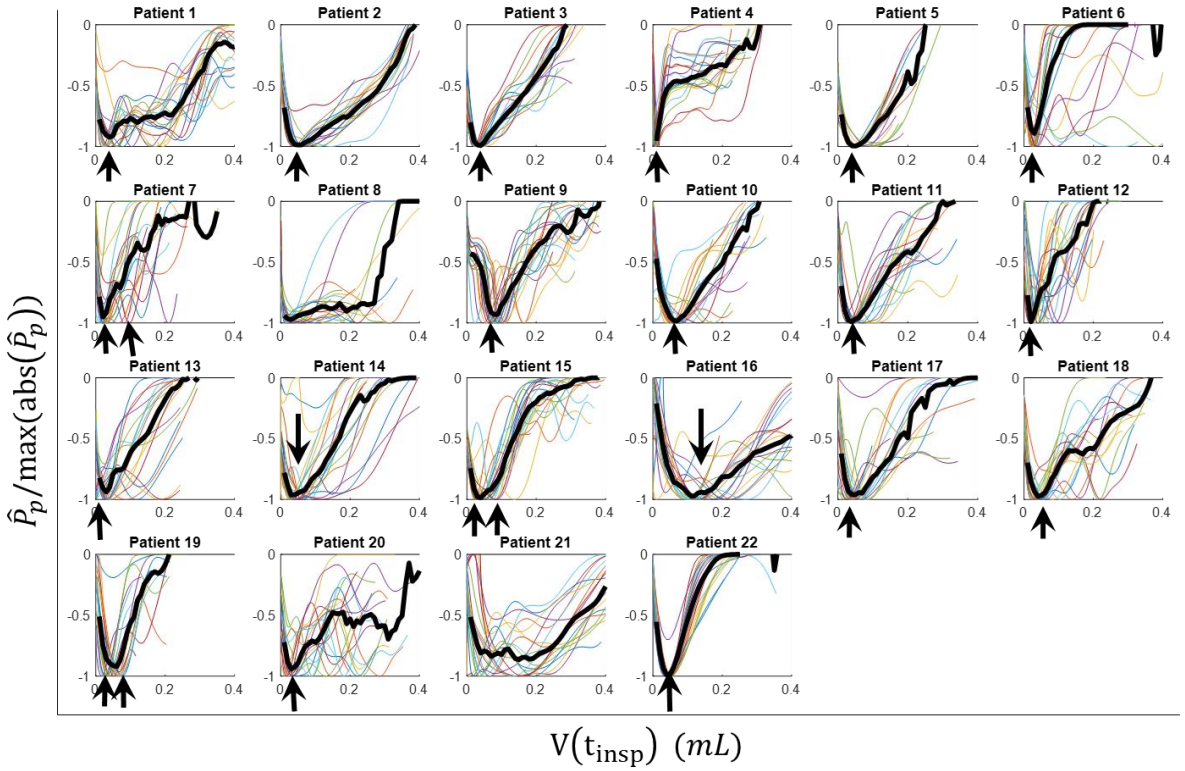

Figure 5: (Normalised) negative pressure generation ($\hat{P}_p$) vs. volume over inspiration for all 22 patients. Each line represents the time course over patient-led inspiration (i.e. to maximum Eadi) for each of the 20 NAVA breaths studied, while the bold line is the median over all 20 breaths. $\hat{P}_p$ is smoothed with a 10 point moving average to remove noise. Arrows indicate locations where the greatest negative pressure generation falls consistently within a small volume range.

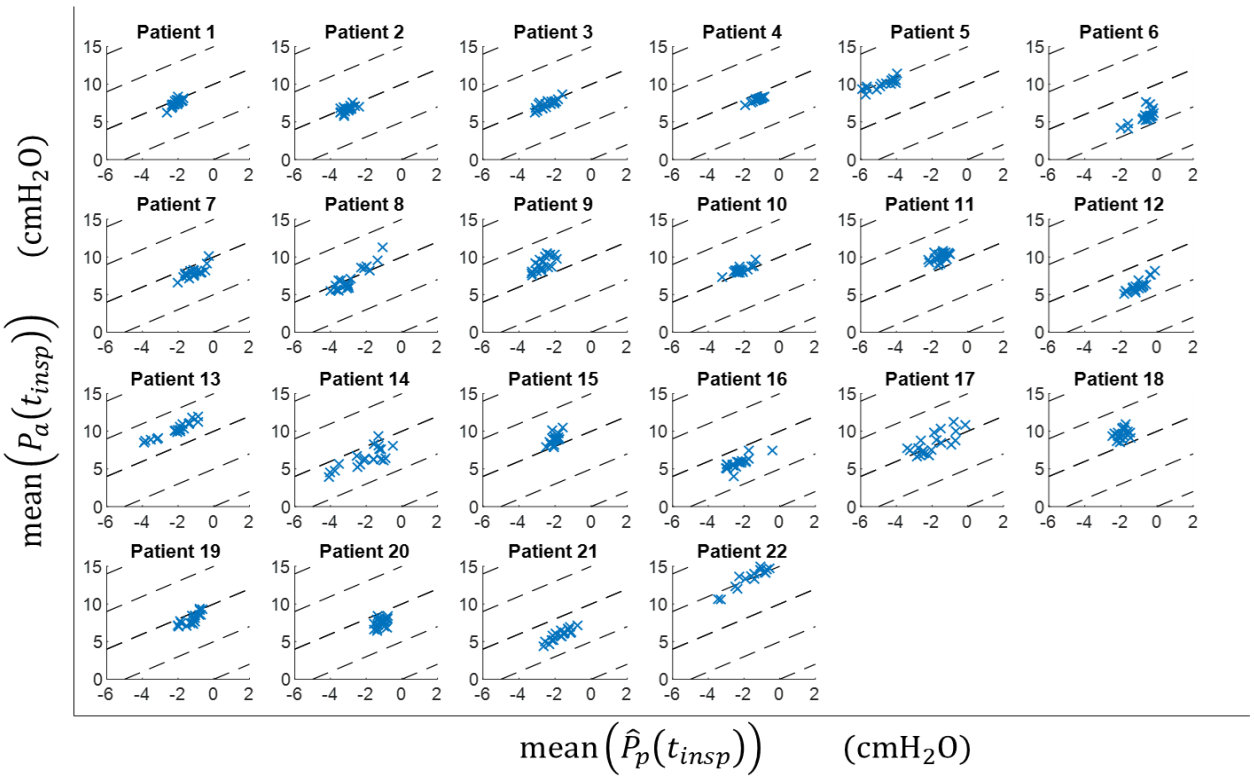

Figure 6: Inspiratory drive vs. alveolar pressure. Dashed lines represent constant trans-pulmonary pressure. Adapted from [37]

Table 1: Ventilation characteristics for 20 breaths under NAVA ventilation. Characteristics are median interquartile [25th – 75th] range as appropriate.

	Patient	RR (1/min)	Vt Med [IQR] (mL)	PEEP (cmH_2O)	T_{insp} Med [IQR] (sec)	T_{exp} Med [IQR] (sec)	PIP breath-breath Med [IQR] (cmH_2O)	Peak Eadi breath- breath Med [IQR]
Brussels	1	12.8	0.6 [0.6 - 0.7]	7.2	1.21 [1.13 - 1.28]	3.39 [3.31 - 3.70]	22.4 [21.5 - 23.9]	635 [601 - 716]
	2	31.9	0.4 [0.4 - 0.5]	5.4	0.74 [0.67 - 0.81]	1.18 [1.03 - 1.28]	21.2 [19.5 - 24.8]	417 [359 - 466]
	3	20.1	0.4 [0.4 - 0.4]	7.3	0.73 [0.70 - 0.76]	2.19 [1.96 - 2.37]	23.8 [21.8 - 25.6]	1407 [1237 - 1561]
	4	20.9	0.3 [0.3 - 0.3]	8.9	1.27 [1.16 - 1.38]	1.55 [1.45 - 1.63]	11.1 [10.5 - 11.7]	348 [304 - 392]
	5	48.1	0.3 [0.3 - 0.3]	11.8	0.46 [0.43 - 0.50]	0.77 [0.73 - 0.83]	30.2 [27.2 - 33.5]	1947 [1617 - 2268]
	6	29.5	0.5 [0.5 - 0.5]	4.4	0.72 [0.70 - 0.78]	1.28 [1.22 - 1.37]	16.0 [14.4 - 17.0]	2873 [2483 - 3117]
	7	20.2	0.3 [0.3 - 0.4]	7.6	0.75 [0.71 - 0.82]	1.72 [1.54 - 2.42]	20.9 [18.4 - 24.5]	946 [780 - 1193]
	8	24.2	0.3 [0.3 - 0.5]	7.5	0.92 [0.82 - 0.98]	1.64 [1.38 - 1.69]	13.6 [11.6 - 18.5]	442 [324 - 691]
	9	20.6	0.5 [0.4 - 0.5]	8.2	1.06 [1.00 - 1.12]	1.86 [1.78 - 2.00]	32.2 [29.2 - 35.3]	290 [269 - 312]
	10	30.7	0.4 [0.4 - 0.4]	8.6	0.71 [0.65 - 0.75]	1.21 [1.19 - 1.31]	21.6 [20.5 - 23.3]	2826 [2454 - 3182]
	11	29.3	0.4 [0.4 - 0.5]	8.6	0.65 [0.58 - 0.72]	1.43 [1.27 - 1.54]	24.7 [22.4 - 27.9]	812 [675 - 886]
	12	24.4	0.3 [0.3 - 0.3]	5.4	0.79 [0.67 - 0.84]	1.68 [1.58 - 1.74]	18.7 [16.4 - 20.8]	1294 [1111 - 1559]
	13	44.7	0.5 [0.4 - 0.5]	10.7	0.47 [0.44 - 0.50]	0.84 [0.78 - 0.88]	27.2 [26.3 - 28.7]	1497 [1317 - 1705]
Geneva	14	14.6	0.4 [0.4 - 0.6]	6.2	0.81 [0.76 - 0.92]	3.19 [2.55 - 3.94]	22.6 [18.3 - 26.2]	985 [710 - 1196]
	15	10.9	0.5 [0.5 - 0.6]	8.2	0.94 [0.86 - 1.01]	4.39 [4.05 - 5.07]	30.9 [28.9 - 32.6]	890 [824 - 965]
	16	20.5	0.6 [0.6 - 0.7]	5.4	0.92 [0.86 - 0.95]	2.07 [1.70 - 2.27]	22.5 [19.8 - 25.1]	1513 [1184 - 1720]
	17	29.2	0.5 [0.4 - 0.6]	7.7	0.69 [0.60 - 0.80]	1.29 [1.04 - 1.58]	20.9 [18.5 - 24.0]	1395 [1129 - 1760]
	18	21.2	0.5 [0.4 - 0.5]	8.2	0.86 [0.80 - 0.92]	1.92 [1.79 - 2.03]	24.1 [22.1 - 26.1]	646 [570 - 729]
	19	26.2	0.3 [0.3 - 0.3]	6.8	0.56 [0.53 - 0.61]	1.72 [1.66 - 1.82]	23.3 [20.8 - 26.5]	418 [357 - 526]
	20	18.7	0.4 [0.4 - 0.5]	5.8	0.87 [0.81 - 0.97]	2.33 [1.81 - 2.76]	20.0 [18.4 - 21.4]	406 [374 - 449]
	21	8.6	0.8 [0.8 - 0.9]	6.0	1.02 [0.97 - 1.18]	5.93 [5.35 - 6.39]	19.2 [18.0 - 20.1]	558 [500 - 611]
	22	45.8	0.4 [0.4 - 0.5]	11.3	0.57 [0.55 - 0.59]	0.72 [0.70 - 0.77]	36.6 [34.6 - 38.8]	5240 [4809- 5549]

PEEP: positive end expiratory pressure; PIP: peak inspiratory pressure; Eadi: electrical activity of the diaphragm

Table 2: Ventilation and model outcomes for n =20 breaths under NAVA ventilation. Characteristics are median [25th – 75th] interquartile range (IQR) as appropriate.

	Patient	E (cmH_20/mL)	R ($cmH_20/mL/min$)	Median RMS (cmH_20)	Driving pressure breath-breath Med [IQR]	Peak Eadi breath- breath Med [IQR] (µV)	Peak $\widehat{P_p}$ breath-breath Med [IQR] (cmH_20)	R^2 PIP vs. Eadi*	R^2 V_t vs. PIP	R^2 $\widehat{P_p}$ vs. Eadi*
Brussels	1	11.5	10.8	0.8	15.2 [14.3 - 16.8]	635 [601 - 716]	-3.8 [-4.1 - -3.7]	0.97	0.84	0.85
	2	25.4	7.2T	0.6	15.8 [14.1 - 19.3]	417 [359 - 466]	-5.3 [-5.7 - -5.1]	0.85	0.93	0.42
	3	18.4	10.7	0.5	16.5 [14.5 - 18.3]	1407 [1237 - 1561]	-4.5 [-4.7 - -4.3]	0.85	0.82	0.53
	4	2.1	0.0	0.2	2.2 [1.6 - 2.8]	348 [304 - 392]	-3.2 [-4.6 - -2.7]	0.24	0.44	0.63
	5	29.8	9.9	0.9	18.4 [15.4 - 21.7]	1947 [1617 - 2268]	-7.9 [-8.8 - -7.3]	0.93	0.83	0.81
	6	9.3	5.9	1.6	11.7 [10.0 - 12.6]	2873 [2483 - 3117]	-1.9 [-2.4 - -1.4]	0.80	0.26	0.59
	7	14.7	13.7	0.8	13.3 [10.8 - 16.9]	946 [780 - 1193]	-2.2 [-2.9 - -1.9]	0.99	0.79	0.76
	8	16.7	5.9	0.7	6.1 [4.1 - 11.0]	442 [324 - 691]	-3.8 [-4.2 - -3.4]	0.99	0.96	0.86
	9	25.4	19.1	0.7	24.0 [21.0 - 27.1]	290 [269 - 312]	-7.3 [-8.2 - -6.0]	0.71	0.49	0.57
	10	14.7	7.6	0.9	13.0 [11.9 - 14.6]	2826 [2454 - 3182]	-4.0 [-4.4 - -3.7]	0.84	0.72	0.69
	11	23.8	7.9	0.5	16.1 [13.9 - 19.3]	812 [675 - 886]	-2.7 [-3.0 - -2.6]	0.92	0.87	0.67
	12	17.4	14.9	1.1	13.3 [11.0 - 15.4]	1294 [1111 - 1559]	-2.2 [-2.9 - -1.9]	0.95	0.64	0.37
	13	12.6	4.8	1.3	16.6 [15.6 - 18.0]	1497 [1317 - 1705]	-3.9 [-4.9 - -3.3]	0.87	0.44	0.47
Geneva	14	14.6	8.4	1.2	16.5 [12.2 - 20.0]	985 [710 - 1196]	-3.8 [-4.9 - -2.9]	0.87	0.72	0.27
	15	16.1	17.9	1.2	22.7 [20.7 - 24.4]	890 [824 - 965]	-4.9 [-5.5 - -4.5]	0.93	0.82	0.44
	16	14.0	6.4	1.9	17.1 [14.4 - 19.7]	1513 [1184 - 1720]	-4.5 [-5.1 - -3.7]	0.87	0.55	0.37
	17	13.6	7.5	1.4	13.2 [10.8 - 16.3]	1395 [1129 - 1760]	-4.6 [-5.5 - -3.2]	0.93	0.72	0.44
	18	20.3	13.1	0.5	16.0 [13.9 - 17.9]	646 [570 - 729]	-4.1 [-4.3 - -3.5]	0.92	0.53	0.70
	19	21.8	17.2	1.7	16.4 [13.9 - 19.6]	418 [357 - 526]	-3.0 [-3.4 - -2.7]	0.96	0.53	0.84
	20	18.4	11.9	0.4	14.2 [12.6 - 15.6]	406 [374 - 449]	-2.2 [-2.5 - -1.9]	0.93	0.60	0.25
	21	6.1	3.9	1.1	13.2 [12.0 - 14.1]	558 [500 - 611]	-3.9 [-4.4 - -3.4]	0.97	0.10	0.35
	22	30.3	11.1	2.3	25.4 [23.4 - 27.5]	5240 [4809- 5549]	-4.0 [-5.1 - -3.7]	0.86	0.47	0.27

PEEP: positive end expiratory pressure; PIP: peak inspiratory pressure; Eadi: electrical activity of the diaphragm

4.0 DISCUSSION

The model presented results in physiologically reasonable negative inspiratory pressure profiles during spontaneous breathing on the NAVA ventilation mode. Model fit to measured data was good (RMS error of 0.9 [0.6 – 1.3] cmH_2O). Finally, the results match known trends with neural signal, Eadi, and trans-pulmonary pressure, where it is important to note Eadi is an entirely independent validation signal in this analysis, as it was not used in the modeling or identification.

Model-identified inspiratory driving pressure in this study captures the relative change in pleural pressure during inspiration, rather than the absolute pressure, where the end-expiration pleural pressure is a function of lung tissue and chest wall properties, as well as the diaphragm and abdominal pressures. The negative inspiratory pressure profiles match pleural or oesophageal pressure shapes and changes in the literature [35-37, 39, 48], including peak negative esophageal pressure before PIP [35, 37, 39, 48] and a net positive change at the end of some breaths [33, 37, 38]. Average trans-pulmonary pressure is consistent across 20 breaths for most patients, as shown in Figure 6, implying consistency in the stress/strain and physiological feedback behaviours. Thus, the shape and magnitude of the inspiratory driving pressures identified here are physiologically plausible, and the model presented here may provide insight into patient breathing effort specific to the PEEP and current context of mechanical ventilation settings.

End-inspiratory effort, with end-inspiration defined as peak Eadi rather than the end of ventilator-delivered flow, was found overall to decrease with increasing peak Eadi. This result matches trends previously observed with increases in NAVA or PS level. Ventilator unloading is well-observed to occur with increasing NAVA [35-37, 49] or PS [29, 33, 34, 50, 51] level, where the higher volumes and/or pressures associated with higher level settings result in lower patient work of breathing, and a greater proportion of the inspired tidal volume delivered by the ventilator. Total unloading, where the

ventilator is observed to carry out the majority of the work of breathing, is patient specific in its pressure setting [33]. In this study, ventilator unloading is seen within a NAVA level, and even within a breath, where larger Eadi signals result in higher ventilator pressure (and thus delivered volume), and the patient reduces or ceases active inspiration as the breath progresses. Thus, a higher linear correlation between end inspiratory effort and Eadi suggests a stronger relationship between muscle activation causing pleural pressure outcomes for a given neural signal, and thus patients with a more consistent breathing effort. Where sedation levels are higher, for example, a lower correlation would be expected. The large number of positive inspiratory driving pressures at peak Eadi in Figure 4, combined with consistency in average trans-pulmonary pressure in Figure 6, implies activation of physiological control systems to avoid over distension and tissue damage.

Imsand et al show similar ventilator unloading within a breath, where for one patient a drop in esophageal pressure is observed early in a breath, followed by a rise to higher than at inspiration-onset near the end of the breath at a trajectory parallel to that in passive breathing. They conclude active inspiration turned to passive inspiration within the same breath [35]. Figure 5 supports this interpretation as it shows for many patients a consistent volume beyond which negative inspiratory effort reduces in magnitude, matching known trends for neuro-mechanical uncoupling with increasing lung volume [49]. This volume is patient, and likely PEEP and NAVA level, specific. In Figure 6 this behaviour corresponds to a consistent trans-pulmonary pressure, which is also proportional to volume (EV). Sinderby et al showed in healthy subjects consistency in trans-pulmonary pressure at different NAVA levels [37], and thus a wider range of inspiratory drives than shown here, and found the iso-transpulmonary pressure differed for quiet breathing and large inspiratory efforts [34].

Some patients showed breath-breath variability around the median achieved inspiratory drive as a function of Eadi input in Figure 3. For example, in Figure 3, Patients 5, 14, and 22 have differing model-

estimated inspiratory driving pressures breath to breath, particularly at their peak pressure generation, for a given Eadi signal. In contrast, Patients 2, 3, and 18, for example, have very consistent pressure generation for a given Eadi input, as well as a consistent volume threshold in Figure 5 and trans-plulmonary pressure in Figure 6, suggesting overall breath-breath consistency in neuromuscular coupling. Patient 8 is also interesting, showing relatively consistent negative inspiratory pressure with Eadi in Figure 3, as well as consistent trans-pulmonary pressure across a range of different alveolar pressures in Figure 6. However, they show no clear volume threshold in Figure 4, but instead maintain high negative pressures even at peak Eadi during most breaths, suggesting that they have not yet reached their threshold for ventilator unloading, and the patient is performing a larger proportion of the WOB. This is supported by the relatively low driving pressures in these breaths, seen in Table 2.

Of patients with variability in model-based inspiratory driving pressure, this variability may not always reflect poor underlying neuro-muscular coupling. For example, both Patient 5 and 22 have good consistency in the volumetric threshold for unloading in Figure 5, as well as in trans-pulmonary pressure in Figure 6, implying consistency in neuromuscular coupling/uncoupling. Patient 5 exhibited the largest model-based inspiratory effort in the cohort, with some negative pressure generations approaching -10 cmH_20, while Patient 22's breathing was asynchronous with the ventilator, with pressure peaks at end-expiration/inspiration-onset despite patient triggering of breaths under NAVA. High residuals in expiration for Patient 22 (Figures 2 and 7) also imply missed dynamics due to active expiration. The variability in pleural pressure may arise from variability in chest wall tension or gastric pressure changes, where activation (or deactivation due to fatigue) of abdominal muscles and/or inter-costal muscles may influence chest wall properties or trans-diaphragmatic pressure, particularly during deep inspiratory drives (Patient 5) or patient-ventilator interactions (Patient 22).

In contrast, Patient 14 showed variability in response across each of Figures 3 – 6, and may thus display fatigue or poor neuro-muscular coupling. Other irregularities were present, as Eadi was erratic during

expiration over several breaths, as show in Figure 7, with occasional false-triggering of breaths, and often displayed a rapid tidal volume drop, followed by a markedly slower decay, during expiration, suggesting underlying issues in breathing triggering and expiratory stiffening. Overall, patients with lower per-patient V_t vs. PIP R^2 values, indicating variability in tidal volume for a given PIP (and thus peak Eadi), also had lower peak $\hat{P}_p|_{peak\ Eadi}$ vs. $Eadi_{peak}$ R^2 values. This suggests that breath-breath neuro-muscular coupling capacity can change, where for a given Eadi two breaths might have differentV_t, and different $\hat{P}_p$, outcomes.

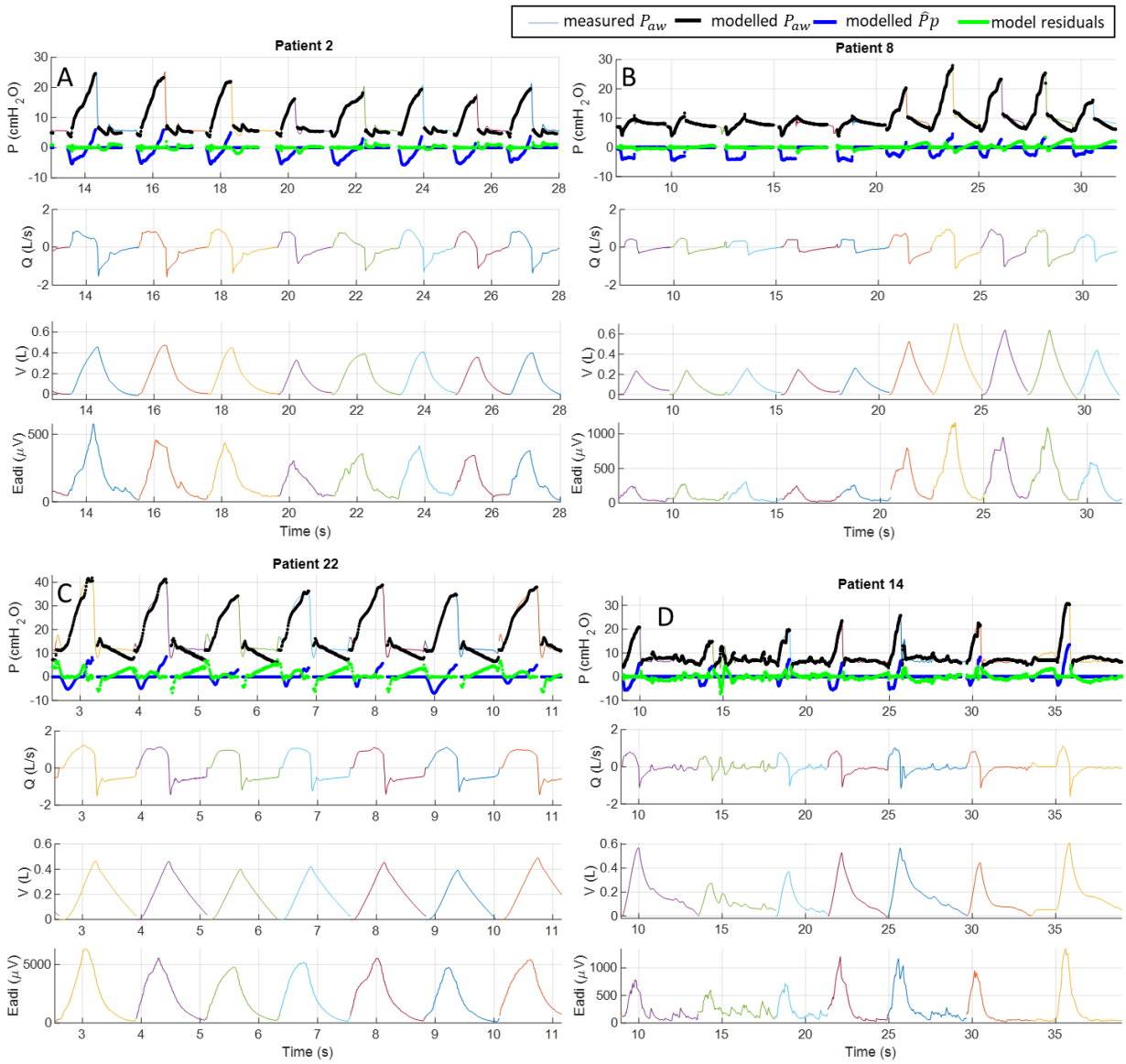

Figure 7: Model fit and measured respiratory profiles for two patients who had: A-B: consistent negative inspiratory pressure for a given Eadi signal (Figure 3), and C-D: significant breath – breath variability in pressure generated for a given Eadi signal (Figure 3).

4.2 Limitations

This model-based analysis of spontaneous breathing effort compares to Eadi and known behaviours for a first validation. A more complete validation would also include comparison to esophageal pressures, which were not available here. However, measurement of esophageal pressure as a surrogate of pleural pressure also has its limitations and may over or underestimate pleural pressure in different contexts [52, 53]. A more precise validation might be obtained by considering an ex-vivo validation experiment using a mechanical model with a known, controlled negative pressure generation input so an exact comparison is possible.

The model presented is likely less effective when ventilator delivered driving pressures are very low, for example in the case of Patient 4 (Table 2, and Figure 2). Model-identified elastance for Patient 4 was very low at 2.1 cmH_20/mL, and resistance was an unphysical 0 cmH_20.s/mL, likely due to parameter trade-off between the elastic properties of the lung (E) and the negative driving pressure. Overall, model residuals are extremely low at 0.2 cmH_20 in Table 2 and Figure 2, suggesting no missing dynamics. Where ventilator delivered driving pressures are higher, a greater proportion of delivered flow/volume is 'passive' and ventilator driven, particularly during expiration, which enables greater differentiation of elastance and breathing effort in parameter identification. Thus, this model is most suited for patients with higher ventilation requirements, and is possibly less useful in patients who are breathing independently and no-longer require invasive mechanical ventilation support.

The model is fit over a series of breaths to ensure passive lung properties (E, R) do not parametrically trade off with inspiratory breathing efforts, ensuring the model is identifiable. Because the trans-pulmonary pressure is a function of the elastance and lung volume ($E*V$), there can be parameter trade off within a breath, and particularly within inspiration. Model fit to multiple breaths, and including expiration, ensures consistent breath-to-breath tissue elastance and airway resistance mechanics, allowing elucidation of the remaining inspiratory drive. A fit over n = 20 breaths was

chosen as a balance between processing time and providing the model with sufficient breaths to clearly estimate breath-breath spontaneous breathing. Model fit over n=50 and n = 100 breaths showed no significant difference in lung mechanics (< 0.1 and 0.4 cmH_2O/mL change in elastance for n = 50 or n=100 breaths respectively, < 0.2 and 0.4 cmH_2O/mL change in resistance, $p>0.78$, see supplementary material) or correlations over the cohort. Thus, the model as presented here is practicable for real-time use at the bedside with a rolling window of 20 breaths, and is robust to the number of breaths used for model fitting.

The model currently constrains the majority of the inspiratory drive to be negative over inspiration. This constraint regularises the optimisation and identifiability problem [54, 55], and thus ensures the optimal model fit is not a b-spline rendition of airway pressure with *E* and *R* set to zero. This constraint means the model as implemented here cannot capture asynchrony at the start of inspiration, or mid-inspiratory coughs or positive pressure generations. Future work should explore minimising the level of regularisation and constraint to ensure an identifiable model with reduced restrictions. Equally, model residuals can be used to identify deviances from expected behaviours, particularly around the start/end of inspiration, to assess asynchrony as measured dynamics not captured by the model as presented, where methods exist to regularise the airway waveforms and quantify asynchrony [21, 56, 57].

CONCLUSIONS

The single compartment lung model was successfully augmented with negative inspiratory drive functions modelled by constrained second-order b-spline basis functions. Average per-patient negative inspiratory driving pressure was -3.9 [-4.5 - -3.0] cmH_2O, with range -7.9 - -1.9 cmH_2O, while average elastance and resistance were 16.4 [13.6 – 21.8] cmH_2O/L and 9.2 [6.4-13.1] $cmH_2O.s/L$ respectively. Most patients showed consistent transpulmonary pressure, despite different peak airway pressures, and a consistent volume threshold beyond which inspiratory drive started to return to zero. As a result, negative inspiratory pressure at peak Eadi (end-inspiration) was often strongly correlated with peak Eadi (R^2=0.25-0.86). Overall, model-based inspiratory drive outcomes align with electrical behaviour, and match trends in literature showing neuro-muscular decoupling as a function of pressure and/or volume. Quantification of patient and ventilator work of breathing contributions may help optimise MV delivery and weaning.

ACKNOWLEGEMENTS & CONFLICTS OF INTEREST

Acknowledgments: The authors wish to gratefully acknowledge the contributions of the following in the collection of the data used here, collected as part of a study of patient-ventilator interaction under NAVA and pressure support: Piquilloud L, Vignaux L, Bialais E, Roeseler J, Sottiaux T, Laterre P-F, Jolliet P, Tassaux D.

Funding: This work was supported by the NZ MedTech Centre of Research Excellence (MedTech CoRE, #3705718).

Conflicts of interest: None.

Ethics approval and consent to participate: Data used in this analysis was collected under informed consent. The study protocol was approved by the ethics committees of both participating centres: the University Hospital of Geneva (Switzerland) and Cliniques Universitaires St-Luc (Brussels, Belgium).

Author contribution: Jennifer Knopp: Conceptualisation, formal analysis and interpretation, writing – original draft, review and editing. Kyeong Tae Kim: Conceptualisation and interpretation. J. Geoffrey Chase: Funding acquisition, conceptualisation, formal analysis, writing – review and editing. Geoffrey Shaw: Clinical insight, writing – review and editing**.**

REFERENCES

1. Slutsky, A.S. and V.M. Ranieri, *Ventilator-induced lung injury.* N Engl J Med, 2013. **369**(22): p. 2126-36.
2. Fan, E., J. Villar, and A.S. Slutsky, *Novel approaches to minimize ventilator-induced lung injury.* BMC Med, 2013. **11**: p. 85.
3. Gattinoni, L., et al., *Physical and biological triggers of ventilator-induced lung injury and its prevention.* Eur Respir J Suppl, 2003. **47**: p. 15s-25s.
4. Parker, J.C., L.A. Hernandez, and K.J. Peevy, *Mechanisms of ventilator-induced lung injury.* Crit Care Med, 1993. **21**(1): p. 131-43.
5. Major, V.J., et al., *Biomedical engineer's guide to the clinical aspects of intensive care mechanical ventilation.* Biomed Eng Online, 2018. **17**(1): p. 169.
6. Chiew, Y.S., et al., *Model-based PEEP optimisation in mechanical ventilation.* BioMed Eng OnLine, 2011. **10**.
7. Rees, S.E., et al., *Using physiological models and decision theory for selecting appropriate ventilator settings.* Journal of Clinical Monitoring and Computing, 2006. **20**(6): p. 421.
8. Sundaresan, A. and J.G. Chase, *Positive end expiratory pressure in patients with acute respiratory distress syndrome - The past, present and future.* Biomedical Signal Processing and Control, 2012. **7**(2): p. 93-103.
9. Brower, R.G., et al., *Higher versus lower positive end-expiratory pressures in patients with the acute respiratory distress syndrome.* N Engl J Med, 2004. **351**(4): p. 327-36.
10. Briel, M., et al., *Higher vs lower positive end-expiratory pressure in patients with acute lung injury and acute respiratory distress syndrome: systematic review and meta-analysis.* JAMA, 2010. **303**(9): p. 865-73.
11. Caironi, P., et al., *Lung opening and closing during ventilation of acute respiratory distress syndrome.* Am J Respir Crit Care Med, 2010. **181**(6): p. 578-86.
12. Halter, J.M., et al., *Effect of positive end-expiratory pressure and tidal volume on lung injury induced by alveolar instability.* Crit Care, 2007. **11**(1): p. R20.
13. Kim, K.T., et al., *Model-based PEEP titration versus standard practice in mechanical ventilation: a randomised controlled trial.* Trials, 2020. **21**(1): p. 130.
14. Amato, M.B., et al., *Driving pressure and survival in the acute respiratory distress syndrome.* New England Journal of Medicine, 2015. **372**(8): p. 747-755.
15. Goligher, E.C., et al., *Effect of Lowering Tidal Volume on Mortality in ARDS Varies with Respiratory System Elastance.* American Journal of Respiratory and Critical Care Medicine, 2021(ja).
16. Lucangelo, U., F. Bernabè, and L. Blanch, *Lung mechanics at the bedside: make it simple.* Current Opinion in Critical Care, 2007. **13**(1): p. 64-72.
17. Bates, J.H.T., *The linear single-compartment model*, in *Lung Mechanics: An Inverse Modeling Approach*, J.H.T. Bates, Editor. 2009, Cambridge University Press: Cambridge. p. 37-61.
18. Morton, S.E., et al., *Predictive Virtual Patient Modelling of Mechanical Ventilation: Impact of Recruitment Function.* Ann Biomed Eng, 2019. **47**(7): p. 1626-1641.
19. Major, V., et al., *Respiratory mechanics assessment for reverse-triggered breathing cycles using pressure reconstruction.* Biomedical Signal Processing and Control, 2016. **23**: p. 1-9.
20. Redmond, D.P., et al., *Evaluation of model-based methods in estimating respiratory mechanics in the presence of variable patient effort.* Computer Methods and Programs in Biomedicine, 2019. **171**: p. 67-79.
21. Chiew, Y.S., et al., *Assessing mechanical ventilation asynchrony through iterative airway pressure reconstruction.* Comput Methods Programs Biomed, 2018. **157**: p. 217-224.
22. Brochard, L., A. Slutsky, and A. Pesenti, *Mechanical Ventilation to Minimize Progression of Lung Injury in Acute Respiratory Failure.* Am J Respir Crit Care Med, 2017. **195**(4): p. 438-442.

23. Gama de Abreu, M., A. Guldner, and P. Pelosi, *Spontaneous breathing activity in acute lung injury and acute respiratory distress syndrome.* Curr Opin Anaesthesiol, 2012. **25**(2): p. 148-55.
24. Verbrugghe, W. and P.G. Jorens, *Neurally adjusted ventilatory assist: a ventilation tool or a ventilation toy?* Respir Care, 2011. **56**(3): p. 327-35.
25. Sassoon, C.S., E. Zhu, and V.J. Caiozzo, *Assist-control mechanical ventilation attenuates ventilator-induced diaphragmatic dysfunction.* Am J Respir Crit Care Med, 2004. **170**(6): p. 626-32.
26. Wrigge, H., et al., *Spontaneous breathing improves lung aeration in oleic acid-induced lung injury.* Anesthesiology, 2003. **99**(2): p. 376-84.
27. Neumann, P., et al., *Spontaneous breathing affects the spatial ventilation and perfusion distribution during mechanical ventilatory support.* Crit Care Med, 2005. **33**(5): p. 1090-5.
28. Kim, K.T., et al., *Quantifying neonatal pulmonary mechanics in mechanical ventilation.* Biomedical Signal Processing and Control, 2019. **52**: p. 206-217.
29. Banner, M.J., R.R. Kirby, and N.R. MacIntyre, *Patient and ventilator work of breathing and ventilatory muscle loads at different levels of pressure support ventilation.* Chest, 1991. **100**(2): p. 531-3.
30. Heulitt, M.J., et al., *Neurally triggered breaths have reduced response time, work of breathing, and asynchrony compared with pneumatically triggered breaths in a recovering animal model of lung injury.* Pediatric Critical Care Medicine, 2012. **13**(3): p. e195-e203 10.1097/PCC.0b013e318238b40d.
31. Piquilloud, L., et al., *Neurally adjusted ventilatory assist improves patient–ventilator interaction.* Intensive Care Medicine, 2011. **37**(2): p. 263-271.
32. Moorhead, K., et al., *NAVA enhances tidal volume and diaphragmatic electro-myographic activity matching: a Range90 analysis of supply and demand.* Journal of Clinical Monitoring and Computing, 2013. **27**(1): p. 61-70.
33. Berger, K.I., et al., *Mechanism of relief of tachypnea during pressure support ventilation.* Chest, 1996. **109**(5): p. 1320-7.
34. Brochard, L., F. Pluskwa, and F. Lemaire, *Improved efficacy of spontaneous breathing with inspiratory pressure support.* Am Rev Respir Dis, 1987. **136**(2): p. 411-5.
35. Imsand, C., et al., *Regulation of Inspiratory Neuromuscular Output during Synchronized Intermittent Mechanical Ventilation.* Anesthesiology, 1994. **80**(1): p. 13-22.
36. Lecomte, F., et al., *Physiological response to increasing levels of neurally adjusted ventilatory assist (NAVA).* Respir Physiol Neurobiol, 2009. **166**(2): p. 117-24.
37. Sinderby, C., et al., *Inspiratory muscle unloading by neurally adjusted ventilatory assist during maximal inspiratory efforts in healthy subjects.* Chest, 2007. **131**(3): p. 711-717.
38. Viale, J.P., et al., *Time course evolution of ventilatory responses to inspiratory unloading in patients.* Am J Respir Crit Care Med, 1998. **157**(2): p. 428-34.
39. Mauri, T., et al., *Esophageal and transpulmonary pressure in the clinical setting: meaning, usefulness and perspectives.* Intensive Care Med, 2016. **42**(9): p. 1360-73.
40. Terzi, N., et al., *Clinical review: Update on neurally adjusted ventilatory assist - report of a round-table conference.* Critical Care, 2012. **16**(3): p. 225.
41. Piquilloud, L., et al., *Neurally adjusted ventilatory assist improves patient-ventilator interaction.* Intensive Care Med, 2011. **37**(2): p. 263-71.
42. Redmond, D.P., et al., *A polynomial model of patient-specific breathing effort during controlled mechanical ventilation.* Conf Proc IEEE Eng Med Biol Soc, 2015. **2015**: p. 4532-5.
43. Langdon, R., et al., *Prediction of high airway pressure using a non-linear autoregressive model of pulmonary mechanics.* Biomed Eng Online, 2017. **16**(1): p. 126.
44. Langdon, R., et al., *Extrapolation of a non-linear autoregressive model of pulmonary mechanics.* Math Biosci, 2017. **284**: p. 32-39.

45. Bates, J., *A Recruitment Model of Quasi-Linear Power-Law Stress Adaptation in Lung Tissue.* Annals of Biomedical Engineering, 2007. **35**(7): p. 1165-1174.
46. Ganzert, S., et al., *Pressure-dependent stress relaxation in acute respiratory distress syndrome and healthy lungs: an investigation based on a viscoelastic model.* Crit Care., 2009. **13**(6): p. R199.
47. Schranz, C., et al., *Hierarchical Parameter Identification in Models of Respiratory Mechanics.* IEEE Trans Biomed Eng, 2011.
48. Piquilloud, L., et al., *Information conveyed by electrical diaphragmatic activity during unstressed, stressed and assisted spontaneous breathing: a physiological study.* Annals of Intensive Care, 2019. **9**(1): p. 89.
49. Beck, J., J. Spahija, and C. Sinderby. *Respiratory Muscle Unloading during Mechanical Ventilation*. 2003. New York, NY: Springer New York.
50. MacIntyre, N.R. and N.E. Leatherman, *Ventilatory muscle loads and the frequency-tidal volume pattern during inspiratory pressure-assisted (pressure-supported) ventilation.* Am Rev Respir Dis, 1990. **141**(2): p. 327-31.
51. Amato, M.B., et al., *Volume-assured pressure support ventilation (VAPSV). A new approach for reducing muscle workload during acute respiratory failure.* Chest, 1992. **102**(4): p. 1225-34.
52. Hedenstierna, G., *Esophageal pressure: benefit and limitations.* Minerva anestesiologica, 2012. **78**(8): p. 959-966.
53. Talmor, D., et al., *Esophageal and transpulmonary pressures in acute respiratory failure.* Crit Care Med, 2006. **34**(5): p. 1389-94.
54. Docherty, P.D., et al., *A graphical method for practical and informative identifiability analyses of physiological models: a case study of insulin kinetics and sensitivity.* Biomed Eng Online, 2011. **10**: p. 39.
55. Bellman, R. and K.J. Åström, *On structural identifiability.* Mathematical Biosciences, 1970. **7**(3–4): p. 329-339.
56. Damanhuri, N.S., et al., *Assessing respiratory mechanics using pressure reconstruction method in mechanically ventilated spontaneous breathing patient.* Comput Methods Programs Biomed, 2016. **130**: p. 175-85.
57. Kannangara, D.O., et al., *Estimating the true respiratory mechanics during asynchronous pressure controlled ventilation.* Biomedical Signal Processing and Control, 2016. **30**: p. 70-78.